

The Climate of the Pacific Arctic

During the First RUSALCA Decade 2004–2013

By Kevin R. Wood,
Jia Wang,
Sigrid A. Salo, and
Phyllis Stabeno

ABSTRACT. The Russian-American Long-term Census of the Arctic (RUSALCA) research program (2004–present) is being conducted during a period of rapid environmental change in the Arctic. With access to both sides of the international convention line, RUSALCA is uniquely positioned to monitor key regions of the Pacific Arctic, including Bering Strait and the western Chukchi Sea. This paper describes the climate context for the first decade of RUSALCA (2004–2013) and provides additional analyses needed to relate observations obtained during three extended research expeditions with seasonal and longer-time-scale variations in sea ice concentration, weather, and ocean temperature patterns in the broader Pacific Arctic region. Results highlight the benefit and continuing need for sustained international and multidisciplinary collaboration in climate research, as exemplified by the RUSALCA program.

Ice-covered seas (Wrangel Island in the background). Photo credit: Marshall Swartz, Woods Hole Oceanographic Institution

INTRODUCTION

The beginning of the Russian-American Long-term Census of the Arctic (RUSALCA) research program in 2004 coincided with a decade of accelerated climate change in the Pacific Arctic. The rapid loss of sea ice during the period from 2004 to 2013 (and continuing to the present day) is the most recognizable characteristic of the emerging “new Arctic” climate (e.g., Carmack et al., 2015). Along with thinning of sea ice, the seasonal timing of melt and freeze has also shifted, especially in the northern Chukchi Sea (Parkinson, 2014; Stroeve et al., 2014; Frey et al., 2015), and there has been an increase in environmental variability, as marked by the record-setting low sea ice events in 2007 and 2012.

This paper describes the climatological context of the RUSALCA decade, along with analyses of seasonal precursor and upstream conditions in the years when extended research expeditions took place: 2004 (July 23–September 6), 2009 (August 30–September 30), and 2012 (July 10–20 and September 1–15). In addition to these expeditions, shorter annual cruises dedicated primarily to mooring operations and repeat hydrography were carried out in Bering Strait and the southern Chukchi Sea (Figure 1). With an operating area covering the whole of the Chukchi Sea including Bering Strait, on both sides of the international convention line, RUSALCA is uniquely able to monitor climate developments in the Pacific Arctic.

Our aim is to provide additional perspective for the results obtained by RUSALCA scientists discussed in this issue, particularly in light of related variations in sea ice cover, summer mean wind field, and ocean surface-layer temperature patterns observed over the RUSALCA decade. By chance, the extended RUSALCA expeditions occurred during a set of three years when summertime conditions in the Chukchi Sea were cooler, for a variety of reasons, from the first to the last cruise, even though the decadal trend in the Pacific Arctic was

clearly in the opposite direction. Given the wide range of seasonal and interannual variability in the operating area, this phenomenon was not unexpected, and it highlights the value of sustained observations provided by oceanographic moorings and other autonomous systems, and for regular multidisciplinary syntheses.

Given limited surface observations, especially in the western Chukchi Sea, we rely on a variety of remote-sensing and retrospective analysis (reanalysis) products. In total, we reviewed 1,500 days of satellite imagery obtained from 2003 to 2014, including sea surface temperature (SST) from the Moderate Resolution Imaging Spectroradiometer (MODIS) on the Aqua and Terra satellites (NASA, 2014) and sea ice concentration from the Special Sensor Microwave Imager (SSM/I) and Imager/Sounder (SSMIS) from the Defense Meteorological Satellite Program (Comiso, 2000). These images are available on the RUSALCA website (<http://www.arctic.noaa.gov/rusalca>). We used the National Oceanic and Atmospheric Administration (NOAA) Optimally Interpolated (OI) SST data set (Reynolds et al., 2007) to map mean SST anomalies, and the National Centers for Environmental Prediction–National Center for Atmospheric Research (NCEP–NCAR) Reanalysis (NNR; Kalnay et al., 1996), the NCEP–Department of Energy (DOE) Reanalysis 2 (Kanamitsu et al., 2002), and the high-resolution North American Regional Reanalysis (NARR; Mesinger et al., 2006) for atmospheric variables.

Variation in summer sea ice concentration is one of the leading factors setting conditions in the upper 10–20 m of the Chukchi Sea and other Arctic marginal seas, especially in the regions once typically covered by thick perennial sea ice (e.g., Timmermans and Proshutinsky, 2014). Annual mean sea ice thickness in the central Arctic Basin has decreased from 3.59 m to 1.25 m since 1975, a 65% reduction (Lindsay and Schweiger, 2015). A lack of ice thick enough to survive the summer melt season naturally

resulted in more open water, especially in the northern and western Chukchi Sea. In this region, primary regulation of the upper ocean environment has shifted from a once relatively stable sea ice-dominated system (Kwok and Untersteiner, 2011) toward one more sensitive to variable meteorological forces, especially wind and waves, and to cloud-cover-mediated solar radiation (Kay et al., 2008; Perovich and Polashenski, 2012; Jeffries et al., 2013; Timmermans, 2015; Wang et al., 2015).

During the RUSALCA decade there was a tendency for higher-than-normal atmospheric pressure to develop over the northern Beaufort Sea in summer (Ogi and Wallace, 2012; Overland et al., 2012). A stronger Beaufort Sea High, in combination with lower pressure over Siberia, referred to as the Arctic Dipole Anomaly (Wang et al., 2009), is linked to an increase in easterly and southerly winds over the Beaufort and northern Chukchi Seas. These winds tend to blow sea ice out of the Chukchi Sea and thus expose a greater fraction of the ocean to solar heating (e.g., Frey et al., 2015). However, year-to-year variations in the summer atmospheric circulation pattern can lead to seemingly contrary results on local and regional scales. In 2012, for example, the Arctic Dipole (and its related wind field) was displaced toward Greenland, and the resulting calm in the Chukchi Sea meant that an unusual amount of sea ice persisted through summer around Wrangel Island and Long Strait, even while a new record was set for low sea ice extent in the Arctic. Fluctuations in the regional wind field also affect flow through Chirikov Basin and Bering Strait (Coachman, 1993; Danielson et al., 2014), with impacts on the upwelling and advection of colder nutrient-rich water northward through the western channel of Bering Strait (Coachman and Shigaev, 1992; Nihoul et al., 1993; Hopcroft and Day, 2013; Grebmeier et al., 2015).

Increasing environmental variability during the summer melt season has a wide range of implications. The changing

pattern of sea ice retreat has not only exposed new ocean areas to increased solar heating but also impacted the potential heating (and illumination) of upper-ocean water parcels as wind and ocean currents transport them over the Bering and Chukchi continental shelves. The result is that an increasing range of variable ocean properties, including SST and heat content, are superimposed on the mean circulation scheme in the northern Bering and Chukchi Seas and beyond (e.g., Coachman et al., 1975; Timmermans, 2015), as best illustrated by the extreme examples of 2007 and 2012. Documented impacts (both positive and negative) of climate change and variability on Arctic marine ecosystems range from altered net primary production and behavior of sea ice-dependent species to the well-being of large marine mammals and seabirds (Arrigo and van Dijken, 2015; George et al., 2015; Kuletz et al., 2015; MacIntyre et al., 2015).

THE ICE-DIMINISHED ARCTIC

Sea ice loss in the northern Bering and Chukchi Seas is part of the continuing Arctic-wide reduction of sea ice extent and thickness observed during the last decade (Polyakov et al., 2012; Lindsay and Schweiger, 2015) that has been accompanied by earlier melt onset in spring and later freeze-up in autumn (Stroeve et al., 2012; Parkinson, 2014; Frey et al., 2015; Wood et al., 2015). Summer sea ice concentrations have declined in most Arctic marginal seas, particularly in areas where multiyear sea ice used to prevail. Reductions of 60–80% in mid-September sea ice concentration have occurred in the northern Chukchi Sea during the RUSALCA decade, compared to the first decade of the satellite era (1980–1989), as shown in Figure 2. The only regions of the Arctic where summer sea ice concentrations are not much reduced are in the central Canada Basin and along the northern coasts of the Canadian Arctic

Archipelago and northern Greenland where quantities of older and thicker multiyear sea ice persist (e.g., Polyakov et al., 2012; Perovich et al., 2014).

The range of year-to-year variability of sea ice concentration in the northern Chukchi and Beaufort Seas (70–80°N) has also changed, from mostly ice-covered (60–87% concentration) in

September during the first decade of the satellite era to mostly open water (5–56% concentration) in 2004–2013 (Figure 2 inset). Only one year, 2006, had sea ice concentrations approximating the 30-year climatological mean (1981–2010); the three RUSALCA expedition years all were $\leq 40\%$ sea ice concentration in this region in September, with 2012 reaching the record minimum of 5% (Wood et al., 2015).

Satellite data also show that mean sea ice concentration from 2004–2013 was lower in the marginal ice zone (north of the 15% concentration limit) during the entire period of retreat, compared to the 1980–1989 period. Sea ice concentrations are 15–30% reduced in the western Chirikov Basin in May, and as the ice retreats northward, this is evident across the region from Long Strait to the eastern Beaufort Sea. Reductions $\geq 40\%$ emerge beyond the shelf break north of Point Barrow in early August and gradually spread into the area of maximum loss shown in Figure 2. This pattern is consistent with earlier onset of melt and retreat in the spring (e.g., Frey et al., 2015) and the nearly complete loss of perennial ice in the northern and western Chukchi Sea (Polyakov et al., 2012). Sea ice reductions in this region remain $\geq 40\%$ until the last part of October, and then gradually disappear as new ice covers the Chukchi Sea.

Reduced sea ice concentrations are an indicator of increased surface heat exchange, facilitated early in the melt season by the lower albedo (reflectivity) of the now predominant first-year ice, and subsequently by the formation of melt ponds and flaw leads (near coasts), and larger open water areas as the season progresses (Perovich et al., 2008; Perovich and

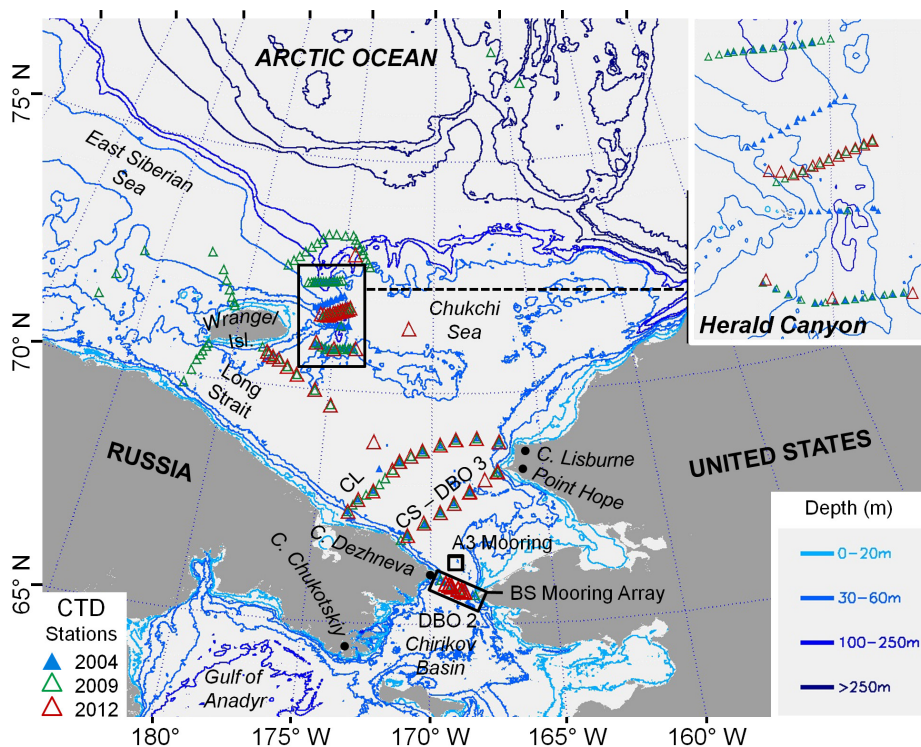


FIGURE 1. The RUSALCA operating area. Conductivity-temperature, depth (CTD) stations occupied during the extended cruises in 2004, 2009, and 2012 are marked with blue, green, and red triangles, respectively. Mooring operations and other research activities were also carried out annually in Bering Strait and the southern Chukchi Sea to the Point Hope to Cape Sherdtse-Kamen' (CS) line (now Distributed Biological Observatory, DBO 3). Details concerning the mooring array can be found in Woodgate et al., 2015, in this issue.

Polashenski, 2012). The delay in freeze-up is related to the additional time required for excess summer heat stored in the surface mixed layer to be either removed to the atmosphere or stored deeper in the water column. This is reflected in large air temperature anomalies that appear over low-ice regions in October (e.g., Wood et al., 2015) and in the near surface temperature maximum (NSTM) at 25–35 m depth in Canada Basin (Jackson et al., 2010; Timmermans, 2015).

There are large year-to-year differences in the way wind and other factors act on the thinner, lower-concentration sea ice, and this contributes to increasing environmental variability in the northern Bering and Chukchi Seas. On the regional scale, this means that cruises may encounter very different conditions from year to year. For example, 2007 and 2012 were both record low sea ice years, but in the latter case, cooler ocean temperatures and unusually high concentrations of sea ice persisted in the RUSALCA operating area around Wrangel Island and Long Strait (e.g., Timmermans et al., 2012).

VARIATIONS IN THE SUMMER WIND FIELD

There has been a tendency for an intensified high-pressure area to form over the northern Beaufort Sea in the summer (June, July, August; JJA) during recent years (Overland et al., 2012; Wood et al., 2013). Winds associated with the Beaufort Sea High, shown in Figure 3, are linked to increased sea ice advection out of the Beaufort and Chukchi Seas, higher air and ocean temperatures, and changes in ocean current patterns (Ogi and Wallace, 2012; Stroeve, et al. 2012; Brugler et al., 2014). There are, however, variations in the development of this pattern each summer, and there are summers when it does not develop at all. Often, the result in these cases has been cooler air and sea temperatures and somewhat more sea ice present through the season. Local conditions can vary widely, however, which complicates the

task of interpreting limited in situ observations, especially where sharp environmental gradients are present.

Figure 4 presents summer mean sea level pressure (SLP) and wind field for 2004, 2009, and 2012. Figure 5 shows a higher-resolution view of July and August winds in the RUSALCA region, computed using NARR. September winds are shown in Figure 6.

In the summer of 2004, high SLP was located over the Canadian Arctic coast near Banks Island (70°N, 130°W), with low SLP over central Siberia. Mean winds over the RUSALCA region were weak, with light south and southeast winds north of 71°N. NARR shows a light southerly flow (1–3.5 ms⁻¹) prevailed over most of the region in July, with very light wind conditions in Long Strait and east of Wrangel Island. Southerly winds increased slightly

in August to between 2 and 3.5 ms⁻¹.

The SLP distribution in the summer of 2009 most closely matches the climatology of the 2004–2013 decade shown in Figure 3, and resembles the Arctic Dipole Anomaly (Wang, et al., 2009; Overland et al., 2012). Easterly and southerly winds were enhanced over the Beaufort Sea and the northern Chukchi Sea, which helped clear the sea ice from Long Strait and westward, and began to push the ice edge northward toward the Chukchi Borderland. The NARR reanalysis shows the strongest mean winds occurred in July, and ranged between 4.5 and 8.0 ms⁻¹, while in August the winds were negligible except for the northern quadrant near the Chukchi Borderland. Ultimately the sea ice retreated far enough to permit a series of stations to be taken in open ice conditions around 77.5°N, 166.4°W.

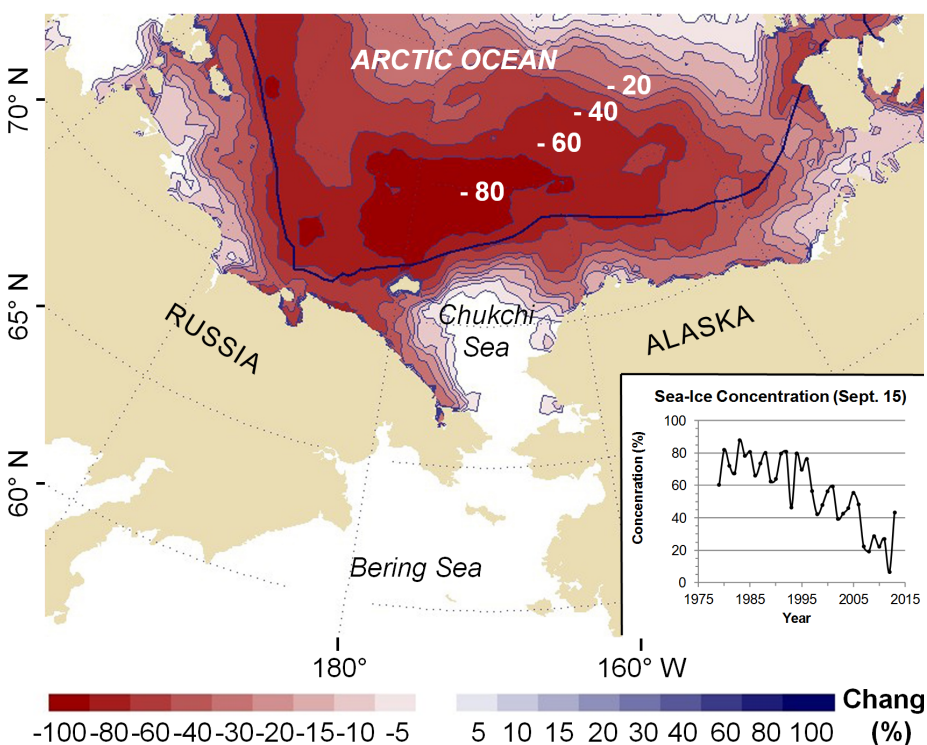


FIGURE 2. Change in sea ice concentration (%) on September 15 for the period 2004–2013, compared to the first decade of the satellite era, 1980–1989, computed using microwave radiometer data (SSM/I and SSM/IS). Summer sea ice concentrations have similarly declined during this period in most of the Arctic marginal seas, with the exception of the zone along the coast of the Canadian Arctic Archipelago and northern Greenland (not shown). Maximum differences occur primarily in regions northward of the former perennial sea ice edge, defined here as the median limit of 90% concentration on September 15, 1980–1989 (heavy blue line). A time series showing the long-term change in mean sea-ice concentration over the corresponding region (70–80°N, 175°E–120°W) is shown in the inset.

Of the three RUSALCA expedition years, the atmospheric circulation of 2012 is the most unusual. The SLP pattern resembles the Arctic Dipole, but it is shifted toward the Atlantic sector. A high-pressure area is centered over Greenland and Iceland, while low SLP is located in Siberia as in other years, but also extends far out into the central Arctic. This is the case in all three months of summer and explains the stronger south and southeasterly winds in the northern Beaufort Sea that contributed to the record low sea ice extent. However, in the western and northern Chukchi Sea, the winds were light and variable, and large amounts of sea ice lingered around Wrangel Island and Long Strait through the summer, even though the main ice pack retreated far to the north

(Timmermans et al., 2012). The progress of the expedition vessel *Professor Khromov* was encumbered by this residual area of sea ice north of Wrangel Island between September 9 and 11.

An exceptionally powerful cyclone also passed across the central Arctic from the East Siberian Sea to the Canadian Archipelago on August 5–12, 2012 (Simmonds and Rudeva, 2012). The contribution of the storm to the record loss of Arctic sea ice in 2012 was ultimately found to be modest, although wind-induced upward mixing of warm subsurface water briefly doubled the rate of ice volume loss in the central Arctic. Chukchi Sea SSTs were further reduced by mixing with cooler deep waters (Zhang et al., 2013; Timmermans and Proshutinsky, 2014).

In September, the wind regime in the

Chukchi Sea and Bering Strait regions switches to prevailing northerlies (Figure 6). There have only been two cases since 1948 when the monthly mean wind in September was not out of the north: 1977 and 2010. Interestingly, the northerly winds during the 2012 RUSALCA cruise were among the strongest shown by NNR and NCEP-DOE (R2) Reanalysis (Kanamitsu et al., 2002) since 1948 and 1979, respectively, and September 2009 was a close second, yet there was little effect on Bering Strait throughflow velocity, reinforcing the notion that remote drivers, such as the Pacific Arctic pressure head gradient, govern during this period (e.g., Woodgate et al., 2005; Danielson et al., 2014; Seth Danielson, University of Alaska Fairbanks, *pers. comm.*, July 16, 2015).

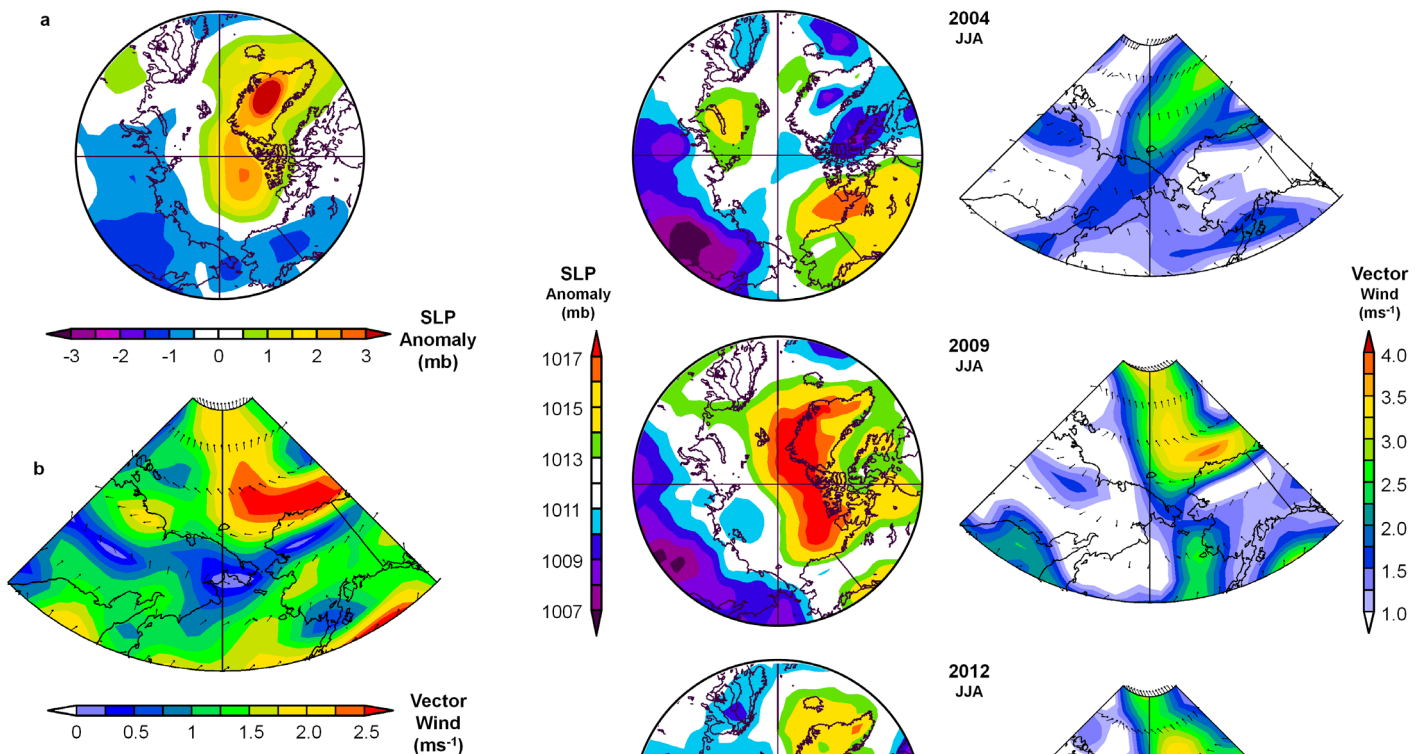


FIGURE 3. (a) Summer (June–July–August, JJA) sea level pressure (SLP) anomaly, and (b) 1,000 mb mean vector wind for the RUSALCA decade (2004–2013) compared to the standard 30-year climatology (1981–2010), as shown by the NCEP-NCAR Reanalysis (Kalnay et al., 1996). The pressure pattern shown here is present throughout the depth of the troposphere and is not limited to the marine boundary layer (Wood et al., 2015).

FIGURE 4. SLP anomaly and mean vector wind for the summer months (JJA) in 2004, 2009, and 2012 (the years extended RUSALCA expeditions occurred), as shown by the NCEP-NCAR Reanalysis.

OCEAN TEMPERATURE PATTERNS

Satellite-derived SST patterns show the combined effects of solar radiation, heat advection by ocean currents and winds, ocean stratification and color, and changing sea ice distribution through the seasonal cycle (Timmermans and Proshutinsky, 2014). Remote sensing provides one of the few opportunities to obtain high-resolution images of SST and other variables across the region, but visible and infrared channels are limited to clear-sky conditions that are not common during the Arctic summer. However, even though the number of cloud-free images is low, it is possible to identify many ocean features in the RUSALCA region, observe how they evolve during the summer, and how they vary from one

season to the next. The NOAA OI SST data set (Reynolds et al., 2007) provides a less-constrained but lower-resolution view of SST in the Bering and Chukchi Seas. These data show that, on the basis of August monthly mean SST anomaly (from 1981–2010 climatology), 2004 was the warmest of the three extended RUSALCA expedition years and 2012 the coolest (and for the 2004–2013 decade). However, positive SST anomalies are present in all three years in areas of maximum sea ice loss north of $\sim 73^\circ\text{N}$, including 2012 (see Timmermans and Proshutinsky, 2014).

The seasonal development of SST patterns for the RUSALCA expeditions are represented by MODIS SST–True Color composite images for each of three expedition years. The images are produced

using a combination of multiple satellite passes and several sensor channels. SST is computed by averaging over a three-day window to reduce the potential impact of cloud shadow and diurnal warming, for example, on the ocean surface skin temperature measured by satellite at a depth of $\sim 10\text{--}20\ \mu\text{m}$ (Donlon et al., 2007). The relationship between skin temperature and subsurface temperature is complex, and differences can exceed 1 K and occasionally 6 K under highly stratified conditions during very calm wind conditions ($<1\ \text{ms}^{-1}$) in daytime (Gentemann et al., 2008; Eastwood et al., 2011; Kilpatrick et al., 2015). In situ data are needed to determine the precise relationship between skin temperature and temperatures at other depths in the mixed layer (e.g., Donlon et al., 2007).

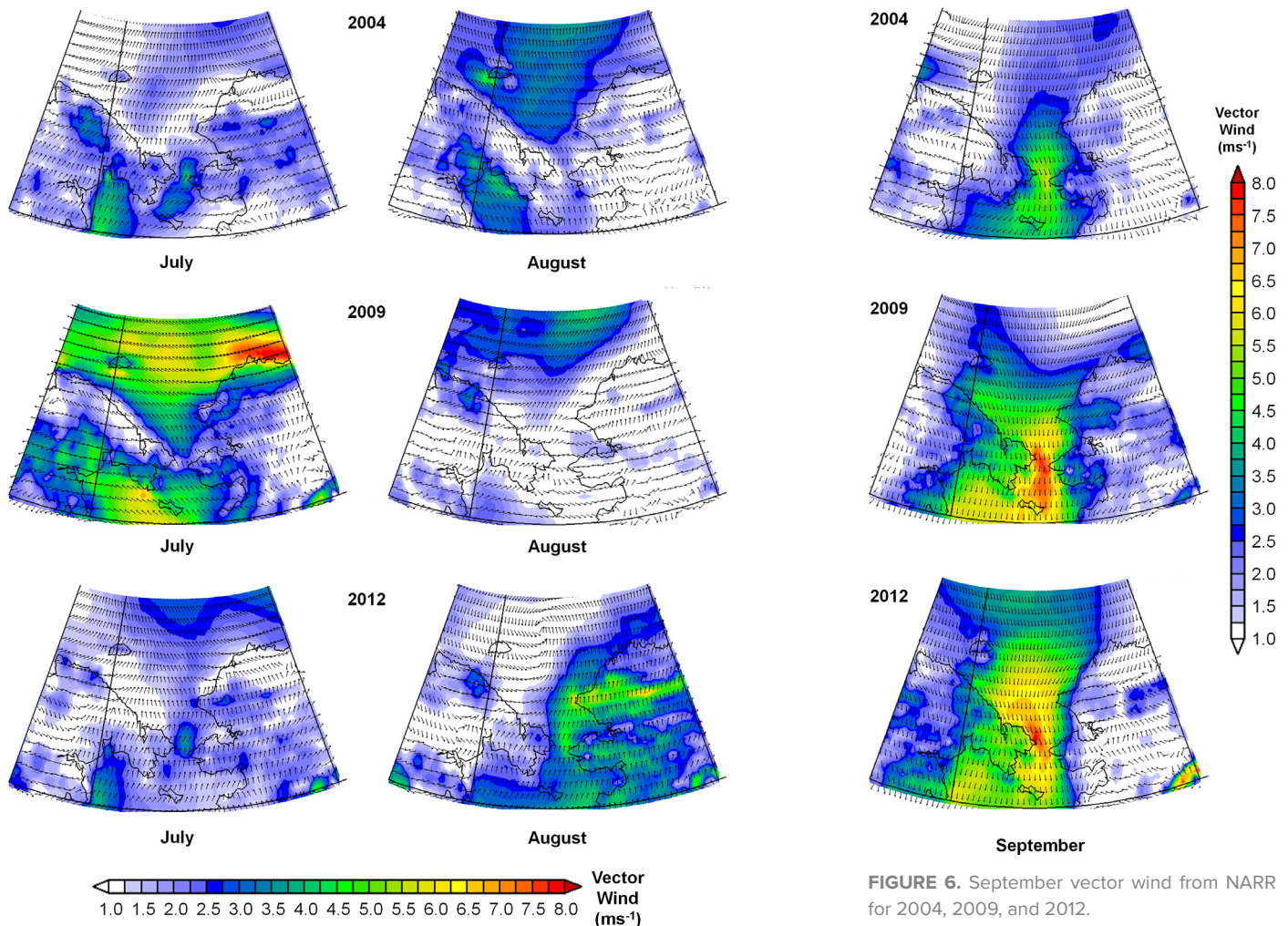


FIGURE 5. July and August vector wind from the high resolution North American Regional Reanalysis (NARR; $0.3^\circ \times 0.3^\circ$) for 2004, 2009, and 2012.

FIGURE 6. September vector wind from NARR for 2004, 2009, and 2012.

In regions of strong mixing and at night, satellite-derived data can provide a reasonable proxy for temperatures below the skin layer (e.g., foundation SST, formerly bulk SST) with the average bias between satellite and collocated drifting buoy data in the range of ± 0.5 K in the upper 1–2 m (e.g., Høyer et al., 2012).

Figure 7 shows images for 2004 and 2009, and Figure 8 provides a set of conductivity-temperature-depth (CTD) transects from 2004 that are coincident

in time, providing an example of collocated satellite and in situ data. Figure 9 shows 2012, which we also compare to 2007 as these two years represent the local extrema of the RUSALCA decade in terms of ocean temperatures and sea ice extent. Images were selected based on the availability of a low cloud-cover window and an approximately similar time interval sufficient to illustrate seasonal development though the melt season in each year. SST is depicted in false color, while

land areas, rivers, clouds, and sea-ice are shown in true color in order to provide better visual definition between features.

Figure 7 (left) shows the summer of 2004. In late June (Figure 7a), the sea ice had retreated from the southern Chukchi Sea, and over nearly the whole region the ocean surface warmed to between 5° and 12°C . The east-west distribution of SST is consistent with the three principal water masses flowing through Bering Strait identified by Coachman et al. (1975): the warmest temperatures associated with Alaskan Coastal Water on the eastern side and the coldest with Anadyr Water on the west, followed by Bering Sea Water in the middle. Cold SSTs associated with upwelling plumes near Cape Dezhneva and Cape Chukotskiy can also be seen (Coachman and Shigaev, 1992; Nihoul et al., 1993; Kostianoy et al., 2004; Walsh et al., 1989b).

The impact of sea ice retreat in the northern and western Chukchi Sea on the development of SST patterns later in the season is readily apparent between late June (Figure 7a) and mid-August (Figure 7c). The well-known embayments in the ice edge associated with the canyons and shoals on the northern Chukchi continental shelf match to a certain extent the SST pattern later in the season, in part due to the persistence of sea ice over the shoals (Bockstoe, 1986; Martin and Drucker, 1997).

In the western Chukchi Sea, the ice edge remained quasi-stationary from the vicinity of Herald Canyon and the Siberian coast between Kolyuchin Bay and Cape Schmidt for the whole of July. The result was a sharply defined north-south temperature front along a similar line, caused primarily by the difference in solar radiation absorbed in the surface mixed layer in the ice-free area. In Figure 7c, cold SSTs linked to the intermittent Siberian Coastal Current (Weingartner et al., 1999) are seen. In 2004, therefore, the ocean surface area susceptible to atmospheric warming was likely constrained by the relatively slow retreat of the sea ice.

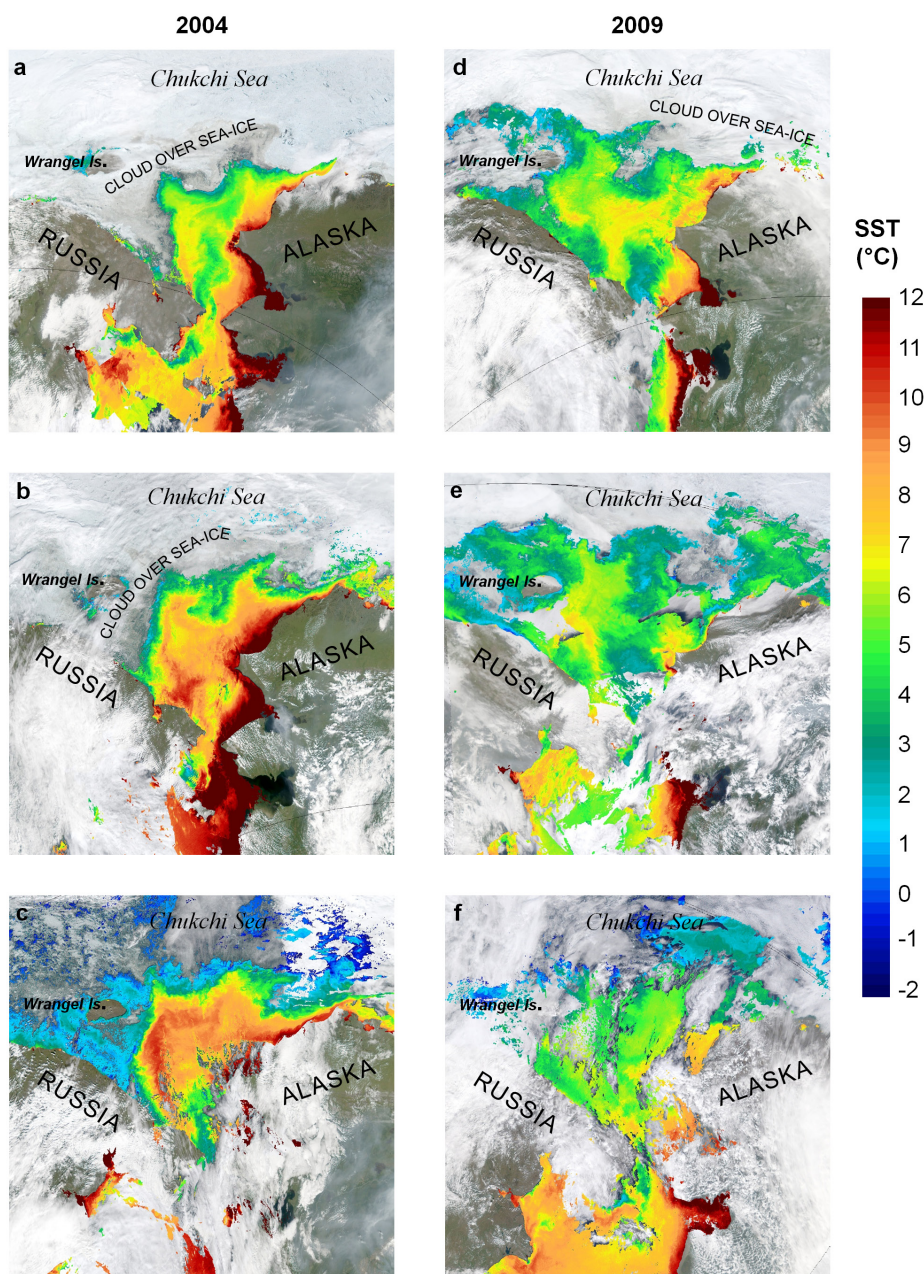


FIGURE 7. (left) MODIS SST–True Color composite images for 2004. (a) June 28–July 1. (b) July 22–25. (c) August 14–17. (right) MODIS SST–True Color composite images for 2009. (d) July 11–13. (e) July 23–28. (f) August 22–24.

Vertical structure related to the 2004 SST pattern in Figure 7c can be inferred from the set of CTD sections in Figure 8. The sections were taken on lines from Cape Lisburne to near Kolyuchin Bay (CL); Point Hope to Cape Sherdtse-Kamen' (CS), also now corresponding to the Distributed Biological Observatory Line 3 (DBO 3); and across Bering Strait (BS). These data suggest the surface mixed layer in the Chukchi Sea was then 10–20 m deep, but warm temperatures (6–10°C) reach to the bottom near the coast of Alaska. Warming of the surface layer to ~10 m observed on the CL section in early July 2014, along with the results of a recent comprehensive analysis of pan-Arctic mixed-layer depth properties by Peralta-Ferriz and Woodgate (2015), suggest that satellite-derived three-day composite SSTs are a reasonable proxy for ~20% of the water column in the Chukchi Sea through much of the summer season, at least for descriptive purposes (see also Coachman et al., 1975).

In 2009 (Figure 7, right), in contrast to 2004, the sea ice cleared from the western Chukchi Sea and Long Strait by mid-July, in part due to strong easterly winds (Figure 5), and by the end of the month it had retreated north of 73°N. By mid-September, the ice edge was situated between 75° and 78°N. Around and to the north of Wrangel Island, SSTs reached to between 5° and 6°C—much warmer than 2004—but in the central and southern Chukchi Sea, SSTs were relatively cool. Bottom temperatures measured at the A3 mooring (66.33°N–168.96°W, 56 m depth) ~60 km north of Bering Strait (Woodgate, et al., 2005) were 1–1.5°C cooler in August and September compared to 2004.

In the Chukchi Sea, OI SST data show the coolest August of the decade in terms of monthly mean SST anomaly occurred in 2012. Below normal SSTs were also observed in the East Siberian and Bering Seas, but in the formerly ice-covered region north of Wrangel Island and in the northern Beaufort Sea, where most of the 2012 ice loss occurred, there

were positive SST anomalies of 2–3°C (Timmermans and Proshutinsky, 2014). Cooler ocean temperatures and lingering sea ice around Wrangel Island were partly the result of the shift of the large-scale circulation associated with the Arctic Dipole toward Greenland, as discussed earlier. Enhanced surface mixing due to the strong Arctic cyclone in August contributed to cooler SSTs in the Chukchi Sea (Zhang et al., 2013), but it is notable that the northern Bering Sea was also cooler than normal, suggesting some larger-scale factors related to atmospheric circulation may have been important in this case. In terms of annual mean near-bottom ocean temperature, 2012 was the coolest measured at the

A3 mooring since 1994, with 2009 being next since 2001 (Woodgate et al., 2015, in this issue).

Figure 9 compares SST patterns in 2012 with those of 2007, the warmest year in the Chukchi Sea during the RUSALCA decade, and illustrates the range of surface layer variability encountered. OI SST data also show that there were positive SST anomalies, generally ranging from 2°–5°C, in the whole region from 60°N to the ice edge in all months from June to September 2007. In 2012, the only positive anomalies occurred in August and September north of Wrangel Island (~2°C); otherwise, negative anomalies between –1° and –2°C prevailed. The MODIS images for 2007 are striking

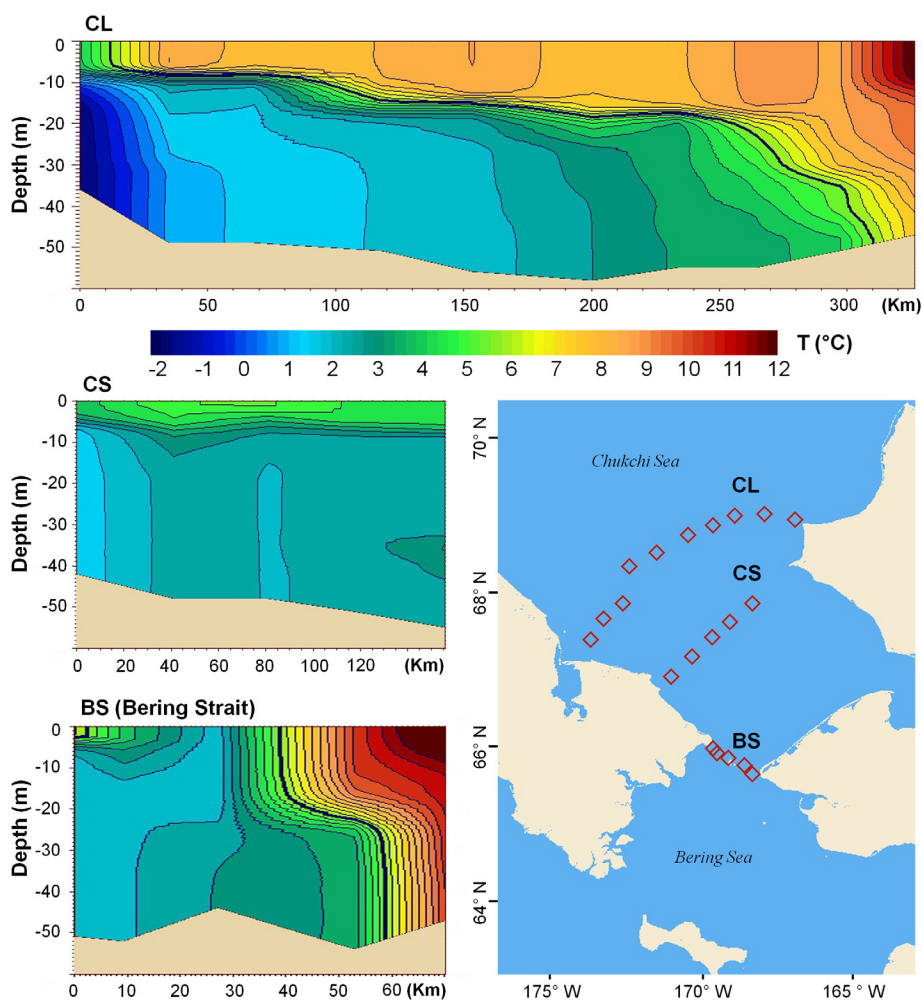


FIGURE 8. CTD sections obtained on the 2004 RUSALCA cruise from August 10–20, corresponding to panel (c) in Figure 7. These data show that satellite-derived SSTs reflect a surface mixed layer depth of 10–20 m, but warm temperatures (6–10°C) reach to the bottom near the Alaskan coast (not shown in the CS line, which ended well offshore). For visual reference, the 6°C isotherm is indicated by the bold line. Station positions are indicated by red diamonds in the map.

for the early and intense warming they depict, with SST values of 8°–12°C everywhere from ~62°–70°N, with the exception of upwelling regions. The upwelling plumes appear to be warmer as well, implying warmer than usual temperatures at depth, but nothing more definitive can be said without further analysis. However, it is notable that Bering Strait mooring data also show warmer near-bottom temperatures in 2007, along with a more rapid increase in

temperature from near freezing on May 1 to 3.3°C on July 31 ($0.06^{\circ}\text{C day}^{-1}$ compared to $0.03^{\circ}\text{C day}^{-1}$ in 2012). Near-bottom temperatures at A3 averaged 2.7°C warmer in July 2007 (maximum 3.5°C) compared to the same period in 2012. SSTs in the Bering Sea south of St. Lawrence Island are also 2–3°C warmer than 2012. Reduced cloud cover in 2007 compared to other recent years is a likely explanation for the anomalous heating over the region (e.g., Kay et al., 2008).

On cloud-free days, direct solar radiation can exceed 300 W m^{-2} (Dong et al., 2010), which can warm a well-stratified surface layer at up to $\sim 0.5^{\circ}\text{C day}^{-1}$ (Wood et al., 2013).

The cold SST signature of upwelling Anadyr Water near Cape Chukotskiy seen in Figures 7 and 9 is also present to some extent in nearly all of the MODIS imagery we reviewed. This feature was described by Walsh et al. (1989a), Nihoul (1986), Nihoul et al. (1993), and others, using a combination of observations, modeling, and satellite remote sensing during the joint US-USSR ISHTAR (Inner Shelf Transfer and Recycling in the Bering and Chukchi Seas) program in the 1980s (McRoy, 1993). Figure 10 shows that the advection of this colder, nutrient-rich plume affects a broad area of the western Chirikov Basin and the southern Chukchi Sea; it is responsible for the high productivity that occurs at DBO 2 (e.g., Kostianoy et al., 2004; Hopcroft and Day, 2013; Grebmeier et al., 2015). The surface expression of the plume varies in extent during the summer and from year to year, as can be inferred from the MODIS composites. The temperature of the plume as it emerges near Cape Chukotskiy also appears to vary by year (i.e., warmer in 2007).

The surface signature of the plume disappears only rarely. Nihoul et al. (1993) suggested this was due to opposing strong north winds, but given the plume is not primarily wind-driven (Deleersnijder, 1994), short-term variations seen in the MODIS imagery may also be caused by the wind-driven advection of warmer and fresher Bering Shelf Water or Alaska Coastal Water over the top of the Anadyr Water (e.g., Gawarkiewicz et al., 1994), obscuring it from the view of satellites. Conversely, in mid-July 1984, the plume was observed in satellite images spread far to the eastward, such that Anadyr Water was apparently present in both channels of Bering Strait (Nihoul, 1986). However, as these variations in the plume arise, they will be reflected in physical and biological characteristics measured in Bering Strait

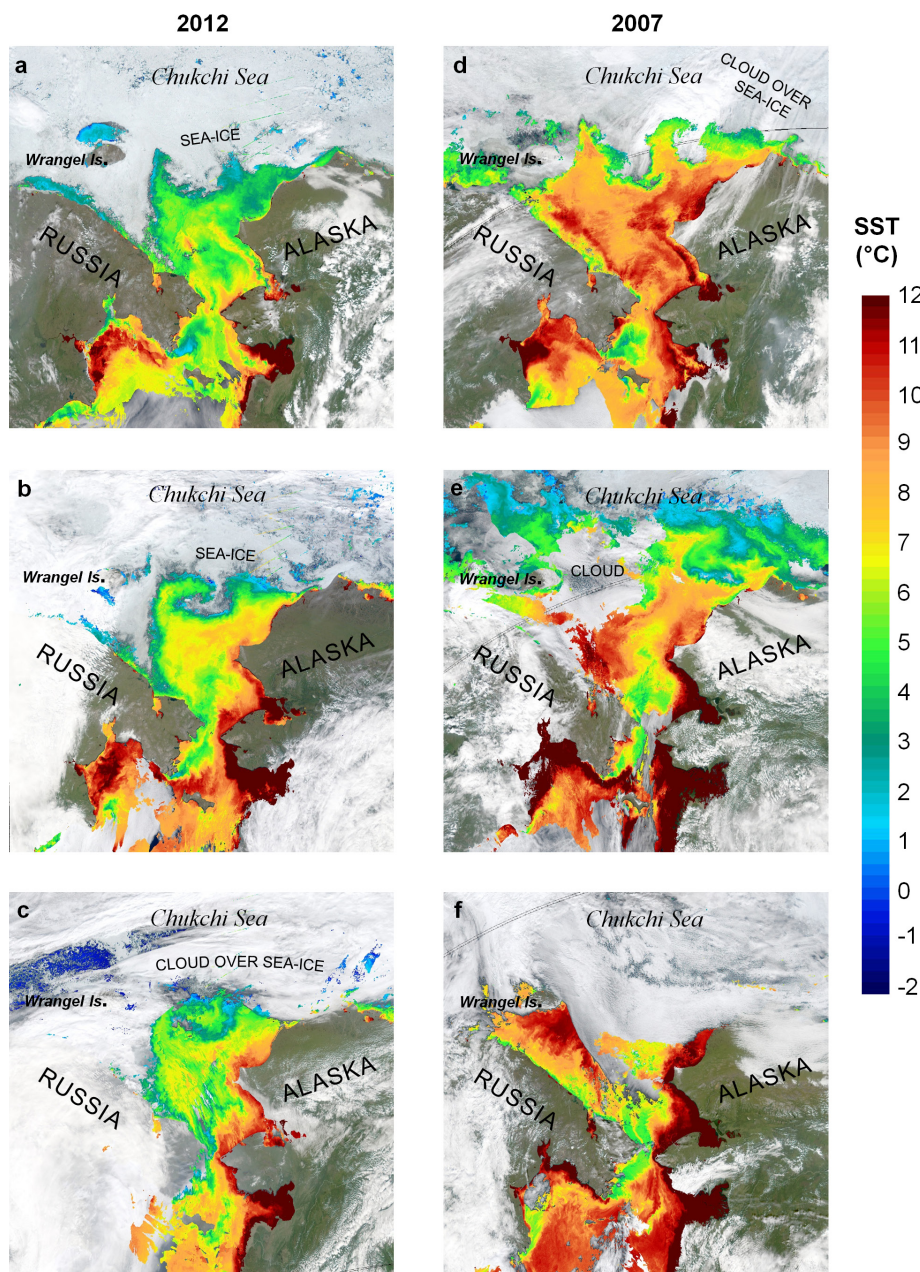


FIGURE 9. (left) MODIS SST–True Color composite images for 2012. (a) July 7–9. (b) July 22–24. (c) August 6–8. (right) MODIS SST–True Color composite images for 2007. (d) July 7–9. (e) July 23–25. (f) August 15–17.

(especially in the western channel) and the Chukchi Sea (e.g., Walsh et al., 1989a; Grebmeier et al., 2015).

DISCUSSION

The RUSALCA program took place during a remarkable period of environmental change in the Arctic. An important feature of these years is the large (and increasing) range of extreme seasons observed in the Pacific Arctic, represented by the large positive ocean temperature anomalies seen in 2007 and the near-record low anomalies in 2012 (e.g., Timmermans and Proshutinsky 2014), and by the long-term change in sea ice concentration in the northern part of the region as shown in Figure 2. In Bering Strait, annual mean transport, near-bottom temperature, and heat flux all followed this pattern (see Figure 5 in Woodgate et al., 2015, in this issue). It is notable that in both 2007 and 2012, minimum summer ice extent records were set, suggesting that the sea ice may now have thinned to the point where a positive anomaly in any of several forcing factors (e.g., winds, surface insolation) may lead to an extreme September sea ice minimum in the Arctic. For the three expedition years, 2004 was the warmest both with respect to mean SST in the Chukchi Sea and the temperature measured at A3, while 2009 and especially 2012 were cooler.

Variations in sea ice concentration and cloud-cover during the melt season help set conditions in the upper ocean in any given year, especially in regions where thick perennial sea ice was once the norm. The regular SST features seen in the MODIS imagery reflect the differential heating of the variously stratified water masses as the season evolves (e.g., Coachman et al., 1975), as determined by cloud-mediated radiation, the pattern and timing of sea ice melt and retreat, river discharge, and upwelling plumes where they occur. In 2004, for example, the persistence of sea ice between Wrangel Island and Siberia, and along the northern shelf break, led to the

formation of a well-defined SST front that was present during the RUSALCA expedition that year. Winds were a factor in clearing sea ice from these areas in 2009, but conversely, a lack of wind and generally cooler ocean temperatures in 2012 contributed to the persistence of a large field of sea ice around Wrangel Island that lingered into September. The more important role of the large-scale atmospheric circulation in 2012 was to bring increased cloudiness and reduced solar

heating to the region during the summer (Overland et al., 2012). Notwithstanding this condition, there were positive SST anomalies of $\sim 3^{\circ}\text{C}$ in the former ice-covered region north of 73°N in the Chukchi and northern Beaufort Seas, where the impact of ice-albedo feedback is greatest.

Comparison between the summers of 2007 and 2012 shows that, for these opposing extreme cases during the RUSALCA decade, the difference in atmospheric warming (as mediated

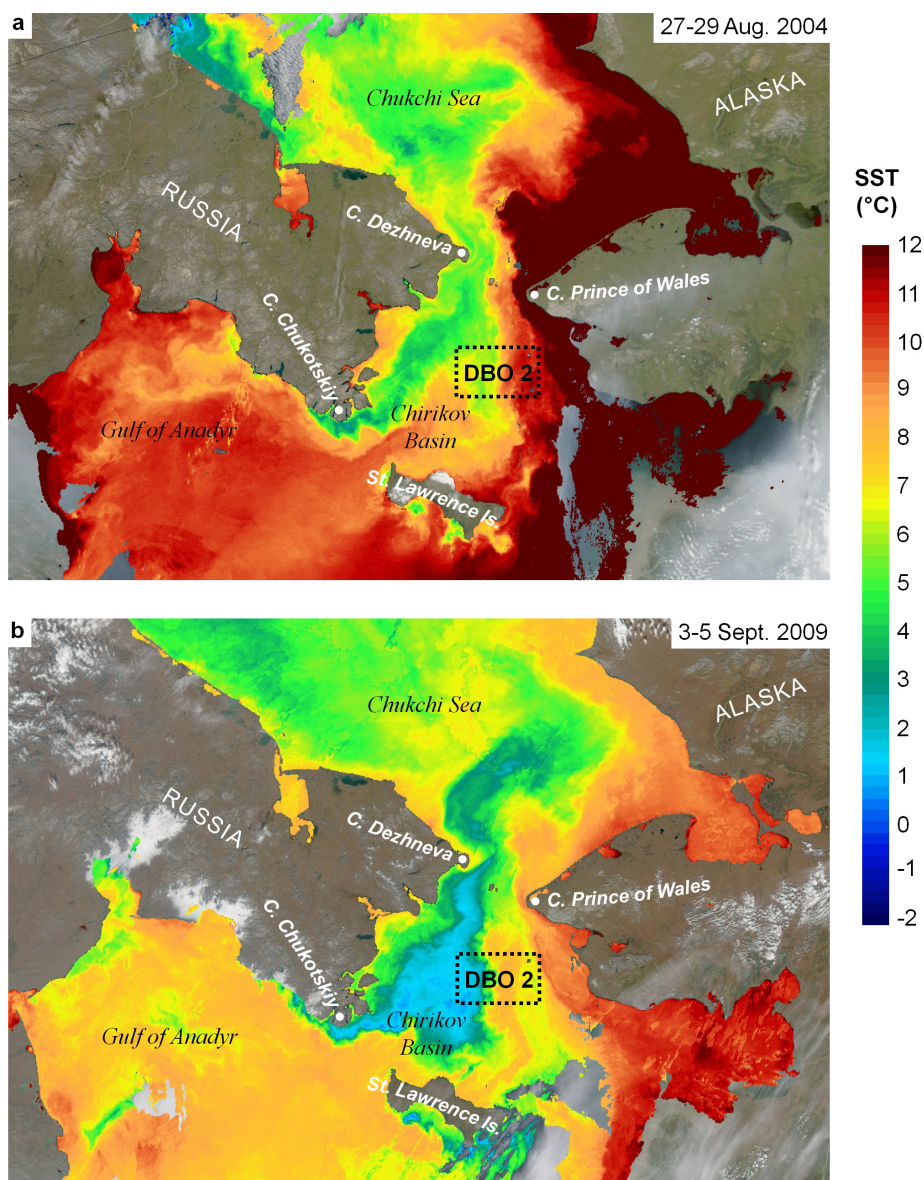



FIGURE 10. The upwelling region in the western Chirikov Basin (a) August 27–29, 2004, and (b) September 3–5, 2009 (MODIS composites as in previous figures). The Anadyr Water plume that emerges near Cape Chukotskiy is ubiquitous in satellite imagery, although it varies widely in extent. It only rarely disappears (Nihoul et al., 1993), but may at times be obscured by advected warm surface layers or by subsequent surface heating. DBO 2 is indicated by the dashed box.

by meteorology and sea ice concentration) was a primary factor driving seasonal variations in the ocean temperature regime in the region. With nearly all of the water that flowed through Bering Strait in summer cooled to near the freezing point of seawater (-1.8°C) the preceding winter, and no anomalously warm ocean water or reduced cloud cover evident south of 62°N in 2007, the pace and amount of subsequent warming must have been initially regulated by differences in surface conditions in the nearby upstream region, for example, in Chirikov Basin and the Gulf of Anadyr. As the sea ice retreated northward across the Chukchi Sea in 2007, the contribution from insolation to ocean heat content also increased compared to ocean advection, supported by reduced cloudiness in the northern part of the region and increased open-water area due to anomalous wind-driven sea ice advection. In Canada Basin, anomalous insolation was the major source of excess heat in the upper ocean (Perovich et al., 2008; Steele et al., 2010; Timmermans, 2015). This stands out in the contrast between the MODIS images from 2007 and 2012 (Figure 9), in particular, in the 2007 intensity of warming over the entire region.

The work accomplished by the RUSALCA program over the last decade in climatological context leads us to the following observations. The sequence of the three long expeditions—in 2004, 2009, and 2012—took place by chance under progressively cooler regional conditions that are not representative of broad-scale and long-term climate trends in the Arctic. They are in, effect, discrete samples from a noisy time series, and understandably liable to aliasing. However, when combined with long-term monitoring provided by mooring arrays, consistent repeat surveys (as provided by the DBO, for example), remote sensing, and reanalysis, the limited ship-based data collections can be appropriately placed in long-term context and synthesized. This argues for the need to maintain long-term multidisciplinary mooring arrays across

Bering Strait and elsewhere in order to work toward increasing autonomous and remote monitoring capabilities that can be deployed for long periods every year in support of RUSALCA and the broader research effort in the Arctic. It also argues for additional focus on regional international and multidisciplinary collaboration in this key region, as exemplified by the RUSALCA program. 

REFERENCES

- Arrigo, K.R., and G.L. van Dijken. 2015. Continued increases in Arctic Ocean primary production. *Progress in Oceanography* 136:60–70, <http://dx.doi.org/10.1016/j.pocean.2015.05.002>.
- Bockstoce, J.R. 1986. *Whales, Ice, and Men: The History of Whaling in the Western Arctic*. University of Washington Press, Seattle, 400 pp.
- Brugler, E.T., R.S. Pickart, G.W.K. Moore, S. Roberts, T.J. Weingartner, and H. Statscewich. 2014. Seasonal to interannual variability of the Pacific water boundary current in the Beaufort Sea. *Progress in Oceanography* 127:1–20, <http://dx.doi.org/10.1016/j.pocean.2014.05.002>.
- Carmack, E., I. Polyakov, L. Padman, I. Fer, E. Hunke, J. Hutchings, J. Jackson, D. Kelley, R. Kwok, C. Layton, and others. 2015. Towards quantifying the increasing role of oceanic heat in sea ice loss in the new Arctic. *Bulletin of the American Meteorological Society*, <http://dx.doi.org/10.1175/BAMS-D-13-00177.1>.
- Coachman, L.K. 1993. On the flow field in the Chirikov Basin. *Continental Shelf Research* 13(5–6):481–508, [http://dx.doi.org/10.1016/0278-4343\(93\)90092-C](http://dx.doi.org/10.1016/0278-4343(93)90092-C).
- Coachman, L.K., K. Agaard, and R.B. Tripp. 1975. *Bering Strait: The Regional Physical Oceanography*. University of Washington Press, Seattle, 172 pp.
- Coachman, L.K., and V.V. Shigaev. 1992. Northern Bering-Chukchi Sea ecosystem: The physical basis. Pp. 448 in *Results of the Third Joint US-USSR Bering & Chukchi Seas Expedition (BERPAC): Summer 1988*. J.F. Turner and P.A. Nagel, eds, US Fish and Wildlife Service, Washington, DC.
- Comiso, J. 2000 (updated 2015). Bootstrap Sea Ice Concentrations from Nimbus-7 SMMR and DMSP SSM/I-SSMIS. Version 2. Boulder, Colorado USA: NASA DAAC at the National Snow and Ice Data Center, http://nsidc.org/data/docs/daac/nsidc0079_bootstrap_seaice.gd.html.
- Danielson, S.L., T.J. Weingartner, K.S. Hedstrom, K. Agaard, R. Woodgate, E. Curchitser, and P.J. Staben. 2014. Coupled wind-forced controls of the Bering–Chukchi shelf circulation and the Bering Strait throughflow: Ekman transport, continental shelf waves, and variations of the Pacific–Arctic sea surface height gradient. *Progress in Oceanography* 125:40–61, <http://dx.doi.org/10.1016/j.pocean.2014.04.006>.
- Deleersnijder, E. 1994. An analysis of the vertical velocity field computed by a three-dimensional model in the region of the Bering Strait. *Tellus A* 46(2):134–148, <http://dx.doi.org/10.1034/j.1600-0870.1994.t01-1-00004.x>.
- Dong, X., X. Baie, K. Crosby, C.N. Long, R.S. Stone, and M.D. Shupe. 2010. A 10 year climatology of Arctic cloud fraction and radiative forcing at Barrow, Alaska. *Journal of Geophysical Research* 115, D17212, <http://dx.doi.org/10.1029/2009JD013489>.
- Donlon, C., N. Rayner, I. Robinson, D.J.S. Poulter, K.S. Casey, J. Vazquez-Cuervo, E. Armstrong, A. Bingham, O. Arino, C. Gentemann, and others. 2007. The Global Ocean Data Assimilation Experiment High-resolution Sea Surface Temperature Pilot Project. *Bulletin of the American Meteorological Society* 88(8):1197–1213, <http://dx.doi.org/10.1175/BAMS-88-8-1197>.
- Eastwood, S., P. Le Borgne, S. Péré, and D. Poulter. 2011. Diurnal variability in sea surface temperature in the Arctic. *Remote Sensing of Environment* 115(10):2,594–2,602, <http://dx.doi.org/10.1016/j.rse.2011.05.015>.
- Frey, K.E., G.W.K. Moore, L.W. Cooper, and J.M. Grebmeier. 2015. Divergent patterns of recent sea ice cover across the Bering, Chukchi, and Beaufort seas of the Pacific Arctic Region. *Progress in Oceanography* 136:32–49, <http://dx.doi.org/10.1016/j.pocean.2015.05.009>.
- Gawarkiewicz, G., J.C. Haney, and M.J. Caruso. 1994. Summertime synoptic variability of frontal systems in the northern Bering Sea. *Journal of Geophysical Research* 99(C4):7,617–7,625, <http://dx.doi.org/10.1029/94JC00259>.
- Gentemann, C.L., P.J. Minnett, P. Le Borgne, and C.J. Merchant. 2008. Multi-satellite measurements of large diurnal warming events. *Geophysical Research Letters* 35, L22602, <http://dx.doi.org/10.1029/2008GL035730>.
- George, J.C., M.L. Druckenmiller, K.L. Laidre, R. Suydam, and B. Person. 2015. Bowhead whale body condition and links to summer sea ice and upwelling in the Beaufort Sea. *Progress in Oceanography* 136:250–262, <http://dx.doi.org/10.1016/j.pocean.2015.05.001>.
- Grebmeier, J.M., B.A. Bluhm, L.W. Cooper, S.L. Danielson, K.R. Arrigo, A.L. Blanchard, J.T. Clarke, R.H. Day, K.E. Frey, R.R. Gradinger, and others. 2015. Ecosystem characteristics and processes facilitating persistent macrobenthic biomass hotspots and associated benthivory in the Pacific Arctic. *Progress in Oceanography* 136:92–114, <http://dx.doi.org/10.1016/j.pocean.2015.05.006>.
- Hopcroft, R.R., and R.H. Day. 2013. Introduction to the special issue on the ecology of the northeastern Chukchi Sea. *Continental Shelf Research* 67:1–4, <http://dx.doi.org/10.1016/j.csr.2013.06.017>.
- Høyer, J.L., I. Karagali, G. Dybkjær, and R. Tonboe. 2012. Multi sensor validation and error characteristics of Arctic satellite sea surface temperature observations. *Remote Sensing of Environment* 121:335–346, <http://dx.doi.org/10.1016/j.rse.2012.01.013>.
- Jackson, J.M., E.C. Carmack, F.A. McLaughlin, S.E. Allen, and R.G. Ingram. 2010. Identification, characterization, and change of the near-surface temperature maximum in the Canada Basin, 1993–2008. *Journal of Geophysical Research* 115, C05021, <http://dx.doi.org/10.1029/2009JC005265>.
- Jeffries, M.O., J.E. Overland, and D.K. Perovich. 2013. The Arctic shifts to a new normal. *Physics Today* 66(10):35–40, <http://dx.doi.org/10.1063/PT.3.2147>.
- Kalnay, E., M. Kanamitsu, R. Kistler, W. Collins, D. Deavens, L. Gandin, M. Iredell, S. Saha, G. White, J. Woollen, and others. 1996. The NCEP/NCAR 40-Year Reanalysis Project. *Bulletin of the American Meteorological Society* 77:437–471, [http://dx.doi.org/10.1175/1520-0477\(1996\)077<0437:TNYRP>2.0.CO;2](http://dx.doi.org/10.1175/1520-0477(1996)077<0437:TNYRP>2.0.CO;2).
- Kanamitsu, M., W. Ebisuzaki, J. Woollen, S.-K. Yang, J.J. Hnilo, M. Fiorino, and G.L. Potter. 2002. NCEP-DOE AMIP-II Reanalysis 2 (R-2). *Bulletin of the American Meteorological Society* 83:1,631–1,643, <http://dx.doi.org/10.1175/BAMS-83-11-1631>.
- Kay, J.E., T. L'Ecuyer, A. Gettelman, G. Stephens, and C. O'Dell. 2008. The contribution of cloud and radiation anomalies to the 2007 Arctic sea ice extent minimum. *Geophysical Research Letters* 35, L08503, <http://dx.doi.org/10.1029/2008GL033451>.
- Kilpatrick, K.A., G. Podestá, S. Walsh, E. Williams, V. Halliwell, M. Szczodrak, O.B. Brown, P.J. Minnett, and R. Evans. 2015. A decade of sea surface temperature from MODIS. *Remote Sensing of Environment* 165:27–41, <http://dx.doi.org/10.1016/j.rse.2015.04.023>.

- Kostianoy, A.G., J.C.J. Nihoul, and V.B. Rodionov. 2004. Frontal zones in the Bering Sea. Pp. 135–189 in *Physical Oceanography of the Frontal Zones in Sub-Arctic Seas*. A.G. Kostianoy, J.C.J. Nihoul, and V.B. Rodionov, eds, Elsevier, Amsterdam.
- Kuletz, K.J., M.C. Ferguson, B. Hurley, A.E. Gall, E.A. Labunski, and T.C. Morgan. 2015. Seasonal spatial patterns in seabird and marine mammal distribution in the eastern Chukchi and western Beaufort Seas: Identifying important pelagic areas. *Progress in Oceanography* 136:175–200, <http://dx.doi.org/10.1016/j.pocean.2015.05.012>.
- Kwok, R., and N. Untersteiner. 2011. The thinning of Arctic sea ice. *Physics Today* 64(4):36–41, <http://dx.doi.org/10.1063/1.3580491>.
- Lindsay, R., and A. Schweiger. 2015. Arctic sea ice thickness loss determined using subsurface, aircraft, and satellite observations. *The Cryosphere* 9(1):269–283, <http://dx.doi.org/10.5194/tc-9-269-2015>.
- MacIntyre, K.Q., K.M. Stafford, P.B. Conn, K.L. Laidre, and P.L. Boveng. 2015. The relationship between sea ice concentration and the spatio-temporal distribution of vocalizing bearded seals (*Erignathus barbatus*) in the Bering, Chukchi, and Beaufort Seas from 2008–2011. *Progress in Oceanography* 136:241–249, <http://dx.doi.org/10.1016/j.pocean.2015.05.008>.
- Martin, S., and R. Drucker. 1997. The effect of possible Taylor columns on the summer ice retreat in the Chukchi Sea. *Journal of Geophysical Research* 102(C5):10,473–10,482, <http://dx.doi.org/10.1029/97JC00145>.
- McRoy, C.P. 1993. ISHTAR, the project: An overview of Inner Shelf Transfer And Recycling in the Bering and Chukchi seas. *Continental Shelf Research* 13:473–479, [http://dx.doi.org/10.1016/0278-4343\(93\)90091-B](http://dx.doi.org/10.1016/0278-4343(93)90091-B).
- Mesinger, F., G. DiMego, E. Kalnay, K. Mitchell, P.C. Shafan, W. Ebisuzaki, D. Jović, J. Woollen, E. Rogers, E.H. Berbery, and others. 2006. North American Regional Reanalysis. *Bulletin of the American Meteorological Society* 87(3):343–360, <http://dx.doi.org/10.1175/BAMS-87-3-343>.
- NASA. 2014. MODIS-Terra Ocean Color Data. NASA Goddard Space Flight Center, Ocean Ecology Laboratory, Ocean Biology Processing Group. http://dx.doi.org/10.5067/TERRA/MODIS_OC.2014.0.
- Nihoul, J.C.J. 1986. Aspects of the northern Bering Sea hydrodynamics. Pp. 385–399 in *Marine Interfaces Ecohydrodynamics*. J.C.J. Nihoul, ed., Elsevier, Amsterdam.
- Nihoul, J.C.J., P. Adam, P. Brasseur, E. Deleersnijder, S. Djenidi, and J. Haus. 1993. Three-dimensional general circulation model of the northern Bering Sea's summer ecohydrodynamics. *Continental Shelf Research* 13:509–542, [http://dx.doi.org/10.1016/0278-4343\(93\)90093-D](http://dx.doi.org/10.1016/0278-4343(93)90093-D).
- Ogi, M., and J.M. Wallace. 2012. The role of summer surface wind anomalies in the summer Arctic sea ice extent in 2010 and 2011. *Geophysical Research Letters* 39:L09704, <http://dx.doi.org/10.1029/2012GL051330>.
- Overland, J.E., J.A. Francis, E. Hanna, and M. Wang. 2012. The recent shift in early summer Arctic atmospheric circulation. *Geophysical Research Letters* 39, L19804, <http://dx.doi.org/10.1029/2012GL053268>.
- Parkinson, C.L. 2014. Spatially mapped reductions in the length of the Arctic sea ice season. *Geophysical Research Letters* 41:4,316–4,322, <http://dx.doi.org/10.1002/2014GL060434>.
- Peralta-Ferriz, C., and R.A. Woodgate. 2015. Seasonal and interannual variability of pan-Arctic surface mixed layer properties from 1979 to 2012 from hydrographic data, and the dominance of stratification for multiyear mixed layer depth shoaling. *Progress in Oceanography* 134:19–53, <http://dx.doi.org/10.1016/j.pocean.2014.12.005>.
- Perovich, D., S. Gerland, S. Hendricks, W. Meier, M. Nicolaus, and M. Tschudi. 2014. Sea ice. In *Arctic Report Card: Update for 2014*. <http://www.arctic.noaa.gov/reportcard>.
- Perovich, D.K., and C. Polashenski. 2012. Albedo evolution of seasonal Arctic sea ice. *Geophysical Research Letters* 39, L08501, <http://dx.doi.org/10.1029/2012GL051432>.
- Perovich, D.K., J.A. Richter-Menge, K.F. Jones, and B. Light. 2008. Sunlight, water, and ice: Extreme Arctic sea ice melt during the summer of 2007. *Geophysical Research Letters* 35, L11501, <http://dx.doi.org/10.1029/2008GL034007>.
- Polyakov, I.V., J.E. Walsh, and R. Kwok. 2012. Recent changes of Arctic multiyear sea ice coverage and the likely causes. *Bulletin of the American Meteorological Society* 93(2):145–151, <http://dx.doi.org/10.1175/BAMS-D-11-00070.1>.
- Reynolds, R.W., T.M. Smith, C. Liu, D.B. Chelton, K.S. Casey, and M.G. Schlax. 2007. Daily high-resolution-blended analyses for sea surface temperature. *Journal of Climate* 20:5,473–5,496, <http://dx.doi.org/10.1175/2007JCLI1824.1>.
- Simmonds, I., and I. Rudeva. 2012. The great Arctic cyclone of August 2012. *Geophysical Research Letters* 39, L23709, <http://dx.doi.org/10.1029/2012GL054259>.
- Steele, M., J. Zhang, and W. Ermold. 2010. Mechanisms of summertime upper Arctic Ocean warming and the effect on sea ice melt. *Journal of Geophysical Research* 115, C11004, <http://dx.doi.org/10.1029/2009JC005849>.
- Stroeve, J.C., T. Markus, L. Boisvert, J. Miller, and A. Barrett. 2014. Changes in Arctic melt season and implications for sea ice loss. *Geophysical Research Letters* 41:1,216–1,225, <http://dx.doi.org/10.1002/2013GL058951>.
- Stroeve, J.C., M.C. Serreze, M.M. Holland, J.E. Kay, J. Malanik, and A.P. Barrett. 2012. The Arctic's rapidly shrinking sea ice cover: A research synthesis. *Climatic Change* 110:1,005–1,027, <http://dx.doi.org/10.1007/s10584-011-0101-1>.
- Timmermans, M.L. 2015. The impact of stored solar heat on Arctic sea ice growth. *Geophysical Research Letters* 42:6,399–6,406, <http://dx.doi.org/10.1002/2015GL064541>.
- Timmermans, M.L., and A. Proshutinsky. 2014. Arctic ocean sea surface temperature. In *Arctic Report Card: Update for 2014*. <http://www.arctic.noaa.gov/reportcard>.
- Timmermans, M.L., A. Proshutinsky, I. Ashik, A. Beszczynska-Moeller, E. Carmack, I. Frolov, R. Ingvaldsen, M. Itoh, J. Jackson, Y. Kawaguchi, and others. 2012. Ocean. In *Arctic Report Card: Update for 2012*. <http://www.arctic.noaa.gov/reportcard>.
- Walsh, J.J., C.P. McRoy, T.H. Blackburn, L.K. Coachman, J.J. Goering, K. Henriksen, P. Andersen, J.J. Nihoul, P.L. Parker, A.M. Springer, and others. 1989a. The role of Bering Strait in the carbon/nitrogen fluxes of polar marine ecosystems. Pp. 637 in *Proceedings of the Sixth Conference of the Comité Arctique International, 13–15 May 1985*. L.R. Rey and V. Alexander, eds, Brill Archive.
- Walsh, J.J., C.P. McRoy, L.K. Coachman, J.J. Goering, J.J. Nihoul, T.E. Whitledge, T.H. Blackburn, P.L. Parker, C.D. Wirick, P.G. Shuert, and others. 1989b. Carbon and nitrogen cycling within the Bering/Chukchi Seas: Source regions for organic matter effecting AOU demands of the Arctic Ocean. *Progress in Oceanography* 22(4):277–359, [http://dx.doi.org/10.1016/0079-6611\(89\)90006-2](http://dx.doi.org/10.1016/0079-6611(89)90006-2).
- Wang, J., J. Zhang, E. Watanabe, M. Ikeda, K. Mizobata, J.E. Walsh, X. Bai, and B. Wu. 2009. Is the Dipole Anomaly a major driver to record lows in Arctic summer sea ice extent? *Geophysical Research Letters* 36, L05706, <http://dx.doi.org/10.1029/2008GL036706>.
- Wang, X., Y. Feng, V. Swail and A. Cox. 2015. Historical changes in the Beaufort-Chukchi-Bering Seas surface winds and waves, 1971–2013. *Journal of Climate*, <http://dx.doi.org/10.1175/JCLI-D-15-01901.1>.
- Weingartner, T.J., S. Danielson, Y. Sasaki, V. Pavlov, and M. Kulakov. 1999. The Siberian Coastal Current: A wind- and buoyancy-forced Arctic coastal current. *Journal of Geophysical Research* 104(C12):29,697–29,713, <http://dx.doi.org/10.1029/1999JC900161>.
- Wood, K.R., N.A. Bond, S.L. Danielson, J.E. Overland, S.A. Salo, P. Stabenro, and J. Whitefield. 2015. A decade of environmental change in the Pacific Arctic region. *Progress in Oceanography* 136:12–31, <http://dx.doi.org/10.1016/j.pocean.2015.05.005>.
- Wood, K.R., J.E. Overland, S.A. Salo, N.A. Bond, W.J. Williams, and X. Dong. 2013. Is there a “new normal” climate in the Beaufort Sea? *Polar Research*, <http://dx.doi.org/10.3402/polar.v32i0.19552>.
- Woodgate, R.A., K. Aagaard, and T.J. Weingartner. 2005a. Monthly temperature, salinity, and transport variability of the Bering Strait through flow. *Geophysical Research Letters* 32, L04601, <http://dx.doi.org/10.1029/2004GL021880>.
- Woodgate, R.A., K. Aagaard, and T.J. Weingartner. 2005b. A year in the physical oceanography of the Chukchi Sea: Moored measurements from autumn 1990–1991. *Deep Sea Research Part II* 52:3,116–3,149, <http://dx.doi.org/10.1016/j.jsr.2005.10.016>.
- Woodgate, R.A., K.M. Stafford, and F.G. Prahl. 2015. A synthesis of year-round interdisciplinary mooring measurements in Bering Strait (1990–2014) and the RUSALCA years (2004–2011). *Oceanography* 28(3):XX–XX, <http://dx.doi.org/XXXX>.
- Zhang, J., R. Lindsay, A. Schweiger, and M. Steele. 2013. The impact of an intense summer cyclone on 2012 Arctic sea ice retreat. *Geophysical Research Letters* 40:720–726, <http://dx.doi.org/10.1002/grl.50190>.

ACKNOWLEDGEMENT

This study is part of the Russian-American Long-term Census of the Arctic (RUSALCA) program, funded in part by the US Department of Commerce, National Oceanic and Atmospheric Administration (NOAA), Arctic Research Program of the Climate Program Office, and the Joint Institute for the Study of the Atmosphere and Ocean (JISAO) under NOAA Cooperative Agreement NA10OAR4320148. JISAO Contribution No. 2468. PMEL Contribution No. 4389.

AUTHORS

Kevin R. Wood (kevin.rwood@noaa.gov) is Research Scientist, University of Washington, Joint Institute for the Study of the Atmosphere and Ocean, Seattle, WA, USA. **Jia Wang** is Research Ice Climatologist/Physical Oceanographer, National Oceanic and Atmospheric Administration (NOAA) Great Lakes Environmental Research Laboratory, Ann Arbor, MI, USA. **Sigrid A. Salo** is a program coordinator at the NOAA Pacific Marine Environmental Laboratory (PMEL), Seattle, WA, USA. **Phyllis Stabenro** is Physical Oceanographer, NOAA PMEL, Seattle, WA, USA.

ARTICLE CITATION

Wood, K.R., J. Wang, S.A. Salo, and P. Stabenro. 2015. The climate of the Pacific Arctic during the first RUSALCA decade: 2004–2013. *Oceanography* 28(3):xx–xx, <http://dx.doi.org/10.5670/oceanog.2015.xx>.